Shape variation in epitaxial microstructures of gold silicide grown on Br-passivated Si(1 1 1) surfaces

S. Chakraborty [a,1], J. Kamila [a,2], B. Rout [a,3], B. Satpati [a], P.V. Satyam [a], B. Sundaravel [b], B.N. Dev [a,*]

[a] Institute of Physics, Sachivalaya Marg, Bhubaneswar 751 005, India
[b] Particle Irradiation Facility, Materials Science Division, Indira Gandhi Centre for Atomic Research, Kalpakkam 603 102, Tamil Nadu, India

Abstract

Kinetic Monte Carlo simulations for growth on substrates of three-fold symmetry predict the growth of islands of various shapes depending on the growth temperature [Phys. Rev. Lett. 71 (1993) 2967]. On Br–Si(1 1 1) substrates growth of epitaxial gold silicide islands of equilateral triangular and trapezoidal shapes have earlier been observed by annealing at the Au–Si eutectic temperature, 363 °C [Phys. Rev. B 51 (1995) 14330]. We carried out annealing with temperature variation within a small window—(363 ± 30) °C. This has led to island growth of additional shapes like regular hexagon, elongated hexagon, walled hexagon and dendrite. Some of the observed island shapes have not been predicted.
© 2003 Elsevier B.V. All rights reserved.

Keywords: Epitaxy; Growth; Halogens; Silicon; Atomic force microscopy; Faceting

1. Introduction

Epitaxial thin films are often grown away from thermodynamic equilibrium and their morphology is influenced by kinetics. The degree to which growth proceeds away from equilibrium dictates to what extent the morphology will be determined by thermodynamic quantities, such as surface and interface free energies, or by the growth kinetics. Atoms deposited on identical substrates under various conditions, up on aggregation, may form islands of several well defined shapes. For example, deposition of submonolayers of Pt on Pt(1 1 1) surfaces leads to triangular islands if the surface temperature is 425 K, while nearly regular hexagons appear if the deposition takes place at 450–470 K; triangles with a different orientation appear for deposition at 550 K and hexagons with three-fold symmetry at 700 K [1,2]. Even vacancies on

[1] Present address: Department of Physics, Bhairob Ganguly College, Kolkata 700056, India.
[2] Present address: Department of Physics, B.J.B. Junior College, Bhubaneswar, Orissa, India.
[3] Present address: Microanalytical Research Centre, School of Physics, University of Melbourne, Parkville, Vic. 3010, Australia.

Pt(1 1 1), produced by missing atoms, aggregate to form hexagonal patterns [3]. The fact that a very small change in the growth temperature can cause a change in shape and the symmetry of the islands is intriguing. Recently, from kinetic Monte Carlo (KMC) simulations Liu et al. [4] identified a kinetic mechanism that leads to triangular island growth and shape changes on surfaces having three-fold symmetry. Their simulations at different growth temperatures suggest that the shape changes observed for Pt/Pt(1 1 1) is likely to be a general process. These have inspired us to explore further, over a temperature window, the growth of gold silicide epitaxial islands on Si(1 1 1), also a substrate with three-fold symmetry, where we earlier observed a shape transition from triangular to trapezoidal island growth [5,6].

Earlier we obtained epitaxial growth of gold silicide on Si(1 1 1) and Si(1 1 0) surfaces by depositing Au on chemically bromine-passivated Si substrates under high vacuum conditions and annealing at the Au–Si eutectic temperature ($T_e = 363$ °C) [5–7]. In this process Si outdiffuses into the Au layer across the interface and forms gold silicide islands [7]. On Si(1 1 1) surfaces we observed the growth of equilateral triangular and trapezoidal epitaxial islands [5,6], where a triangular to trapezoidal shape transition [6] as a function of island size was identified. On Si(1 1 0) surfaces, which have a two-fold symmetry, long parallel wire-like islands with aspect ratio as large as 200:1 was observed [7]. These gold silicide islands are much thicker than the initially deposited Au layer. Si outdiffusion from the substrate into the Au layer and additional surface diffusion of Au lead to the formation of these columnar islands. The lateral diffusion of Au in this system additionally leads to Au–Au aggregation and fractal growth [8].

In the present work we report our study of gold silicide growth on Si(1 1 1) surfaces over an annealing temperature window around the eutectic temperature, T_e. The purpose of this study is to look for other island shapes predicted for growth on substrates of three-fold symmetry.

The case of growth of gold silicide on silicon is not as simple as the metal-on-metal systems. In this case deposited Au does not show regular is-

land formation. Annealing at a particular temperature causes growth of epitaxial islands of gold silicide. As the alloy phase diagram of Au–Si suggests [9], a temperature variation around the eutectic point (363 °C) would complicate the matter by introducing a composition variation. Nevertheless, we observe other shapes (than those observed earlier—triangular, trapezoidal) of islands predicted for growth on a three-fold substrate. In addition we observe growth of some unpredicted (from KMC simulation) features like ring-like walled islands—somewhat like what has recently been observed on Pb islands on Si(1 1 1) and attributed to competing classical and quantum effects in shape relaxation [10].

2. Experiment

We have used a non-UHV method to obtain the Au–Si island structures on Si(1 1 1). The method involves evaporation of gold of thickness ~450 Å (under ~3 × 10⁻⁶ mbar pressure) on to a bromine-passivated commercial n-type Si(1 1 1) wafer [hereafter Br–Si(1 1 1)]. The Si(1 1 1) wafer was symmetric (not vicinal as in our earlier studies [5,6]). Details of the Bromine-passivation technique has been given elsewhere [11,12]. This method of Br-passivation of the Si(1 1 1) surface provides Br adsorption of ~1/4 monolayer at the atop site on the surface Si dangling bonds on the hydrofluoric acid-etched Si(1 1 1) surface. Br adsorption inhibits the surface oxidation process [13]. During deposition of Au the substrate was kept at room temperature. The film was subsequently annealed under high vacuum condition for 30 min within a temperature range, $\Delta T = \pm 30$ °C, around the Au–Si eutectic temperature of 363 °C. The surfaces of the samples were characterized by Atomic Force Microscopy (Nanoscope, Digital Instruments, USA).

3. Results and discussion

We allowed the variation of annealing temperature within ±30 °C of the eutectic temperature. This produces islands of various shapes: regular

hexagon, elongated hexagon, walled hexagon, faceted vacancy islands and dendritic growth. AFM images in Fig. 1 shows regular and elongated hexagons. A height scan along the line
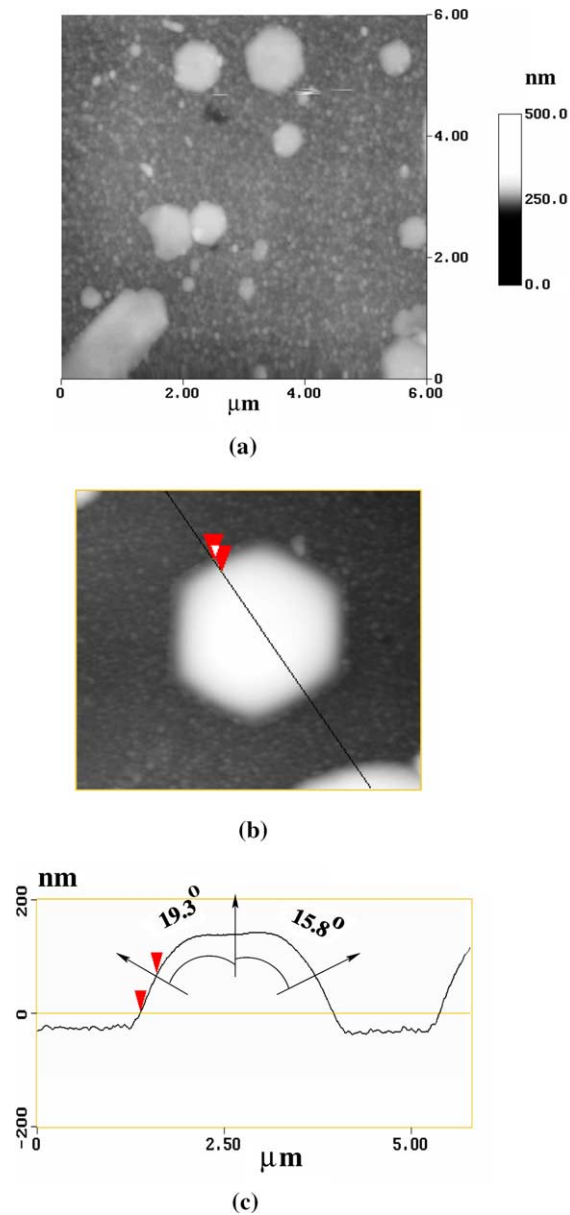

(a)

(b)

(c)

Fig. 1. (a) An AFM scan image shows hexagonal islands grown on a (363 ± 30) °C-annealed Au($\sim$45 nm)/Br–Si(1 1 1) sample surface; (b) one of the hexagonal islands; (c) cross-sectional height scan along the line shown in (b) indicating various facets.

marked in Fig. 1(b) and island facets are shown in Fig. 1(c). The structure of gold silicide in not unambiguously known. Additionally, with the variation of annealing temperature a variation in the composition $Au_{1-x}Si_x$, and possibly the structure is expected from the Au–Si alloy phase diagram [9]. This makes indexing of the facets (Fig. 1(c)) difficult. Without knowing the crystal structure it is not possible to identify the facets. The measured angles between Si[1 1 1] and surface normals of the shown facets are 15.8° and 19.3° (Fig. 1(c)).

Fig. 2(a) shows an AFM image with hexagonal islands having a ring-like wall structure. The cross-sectional height scan around one such island is shown in Fig. 2(b). The center of another ring-like island seen in Fig. 2(a) is even deeper. Around the periphery of the hexagonal islands, the islands
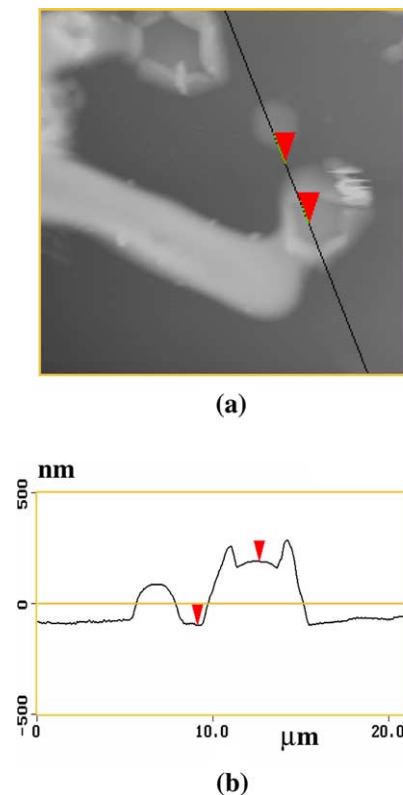

(a)

(b)

Fig. 2. (a) An AFM scan image showing growth of walled-hexagonal islands, (b) a cross-sectional scan along the line indicated in (a).

have grown taller. Such walled islands have not been predicted from KMC simulations of homo-epitaxial growth on three-fold substrates [4]. Recently, growth of hexagonal ring-shaped islands have been reported by Okamoto et al. [10]. They observed transformation of Pb islands on Si from flat top facet geometry into an unusual ring shape. The ring morphology apparently results from the competing classical and quantum effects in the shape relaxation. Surface steps also apparently have a role to play. They claim that the volume-preserving mass transport, that causes the ring morphology, is catalyzed by the electrical field from a scanning tunneling microscope. Of course we cannot compare our case to this. It needs to be further explored as to what leads to such ring-like island growth as seen in our case. Formation of some triangular islands with trenches and walls are also seen (Fig. 3). The island on the left side in Fig. 3 shows a trench–wall–trench–wall–trench structure starting with a trench at the center, while the island on the right follows the same sequence but with an island at the center. Mechanisms of formation of such structures are not yet understood.

Another interesting phenomenon of growth of islands within the perimeter of a vacant region (vacancy island) is observed in Fig. 4. Islands have apparently grown at steps within the vacancy island, spanning several steps.
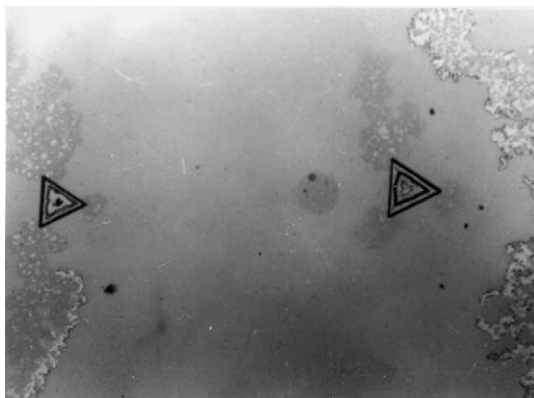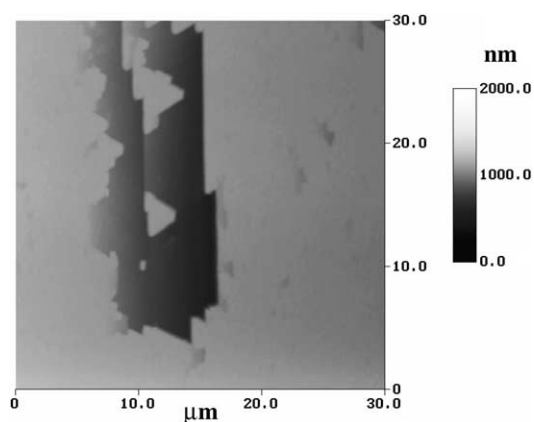

Fig. 4. An AFM micrograph showing islands grown within the perimeter of a large vacancy island or void. Islands apparently span over many steps.

An AFM micrograph is presented in Fig. 5 showing the dendritic growth. Although somewhat different dendritic growth was observed for Pt growth on Pt(1 1 1) which transform into triangular islands in the lower temperature range [4]. We observed fractal growth also for annealing at T_e [8].

In our case growth of islands do not occur directly during deposition, which was performed on substrate at room temperature. Upon annealing, Si from the substrate is supplied to the Au layer via diffusion across the Au/Si interface. Then epitaxial gold silicide grows by reactive epitaxy in a layer-

Fig. 3. An optical micrograph showing triangular islands with wall–trench–wall structure. Field of view of the micrograph corresponds to 400 μm in horizontal direction.
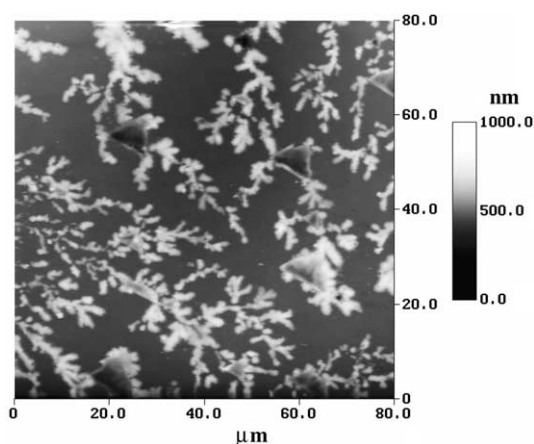

Fig. 5. An AFM micrograph shows dendritic growth.

plus-island or Stranski–Krastanov process [5,6]. The strained epitaxial islands show triangular, trapezoidal shapes as observed earlier [5,6] and hexagonal and ring-like hexagonal shapes as shown here for growth on Si(1 1 1) surfaces, which have a triangular symmetry. These are apparently the general features of growth on substrates of three-fold symmetry.

The feature shown in Fig. 6 was not observed in our earlier experiments with annealing at a constant temperature (T_e). The connected chain of beads on a uniform background reminds one of a phase separation process. Referring to the Au–Si alloy phase diagram [9] we know that the eutectic composition (can be written approximately as Au_4Si) is formed at T_e [5]. If the eutectic composition is written as $Au_{1-x}Si_x$ (C), at $T > T_e$ alloys of compositions $Au_{(1-x)-\delta}Si_{x+\delta}$ (A) and $Au_{(1-x)+\delta}Si_{x-\delta}$ (B) can be formed. Analysis of coarsening in a three-phase multicomponent system, where two low volume fraction phases α and β are present in the γ phase matrix [14] may help in understanding this morphology (Fig. 6). The three-phase simulation [15] of the evolution of microstructure shows the growth of branched chains of connected beads of alternate α and β phase in the continuous γ phase matrix. The branches of connected beads in Fig. 6 have striking similarities with the simulated morphology in Fig. 3 of Ref. [15]. In our case the eutectic phase (C) is dominant [5,6]. Here one

Fig. 6. AFM micrograph showing branches of connected beads. See text for details.

tends to compare the compositions A and B to α and β phases (although A and B may not be clearly defined phases) and speculate that similar physical processes are involved in this microstructure formation. We speculate that the background in Fig. 6 is C and the alternating beads are A and B. These can be confirmed by composition measurements on individual beads with high precision. We do not have access to techniques capable of doing that.

In order to put the present results in perspective, let us discuss the gold silicide formation and the structures briefly. The eutectic composition is $Au_{81.4}Si_{18.6}$. Some reported gold silicides near this composition are $Au_{76.7}Si_{23.3}$ (cubic, $a = 9.60$ Å) [16,17], $Au_{81}Si_{19}$ (cubic, $a = 5.554$ Å) [17,18], Au_3Si or $Au_{75}Si_{25}$ (orthorhombic, $a = 7.82$ Å, $b = 5.5$ Å, $c = 11.16$ Å) [17,19] and $Au_{71}Si_{29}$ ($\sim Au_5Si_2$: hexagonal, $a = 9.38$ Å and $c = 15.46$ Å) [20]. The authors in Ref. [18] have designated the metastable $Au_{81}Si_{19}$ phase as $Au_4Si.m$ phase. Gold silicide growth in Au films on a Si(1 1 1) surface with a composition $Au_{83}Si_{17}$ was observed with a rectangular unit cell with lateral periodicities $a = 9.35$ Å and $b = 7.35$ Å [21]. All these imply that with a small composition variation around the eutectic the unit cell could be cubic, orthorhombic or hexagonal. Earlier we had grown gold silicide on bromine-passivated Si(1 1 1) and Si(1 1 0) surfaces by annealing deposited Au layers at the eutectic temperature [5–7]. This silicide has a composition $Au_{79}Si_{21}$ (with an uncertainty of $\pm 3\%$). We wrote this composition as Au_4Si. We removed the unreacted gold by etching the samples in aqua regia and then performed various experiments to establish the nature of this silicide. X-ray photoelectron spectroscopy measurements showed a chemical shift of Au $4f_{5/2}$, $4f_{7/2}$ and Si $2p$ levels which established gold silicide formation [22]. Previous studies suggested that the peak chemical shifts indicate Au–Si interaction and the presence of a chemical reaction owing to the formation of a gold silicide [23]. We probed the crystallinity of gold silicide by ion channeling experiments, and found its growth to be epitaxial with the underlying substrate [7,24]. The epitaxial growth was already implied in the shape of the gold silicide islands [6]. Currently we are studying growth of nanowires and nanorods of gold silicide on
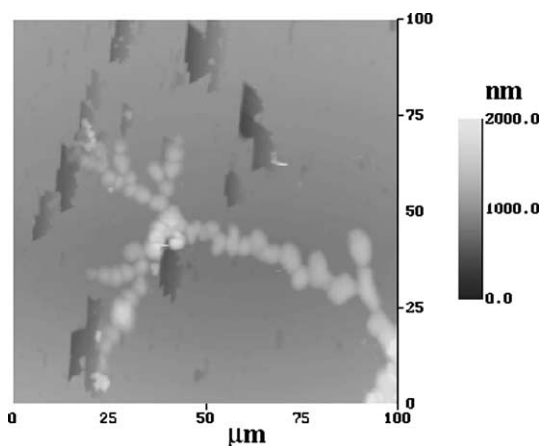
bromine-passivated Si(1 1 0) surfaces by high resolution transmission electron microscopy (HRTEM), the details of which will be published elsewhere. This possibility of nanowire formation was implied in our earlier study where we observed straight wire-like growth of gold silicide with aspect ratios as large as 200:1 [7]. In order to show the formation of gold silicide and its epitaxy beyond any doubt, here we present a typical selected area diffraction pattern and a HRTEM image in Fig. 7. The results in Fig. 7 are for the gold silicide obtained by annealing at the eutectic temperature (T_e). In the present work we allowed the annealing temperature to vary around T_e. This can certainly cause a composition variation and change the structure of the silicide. Interestingly, the 2.26 Å planar spacing seen in Fig. 7 is a common feature
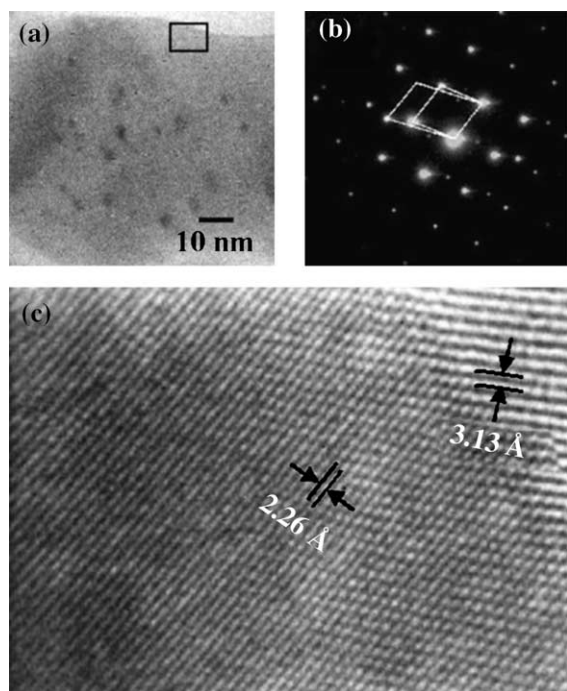

Fig. 7. (a) A bright field image showing a part of a gold silicide island on Si, (b) a selected area diffraction pattern from this area and (c) a plan-view HRTEM image from the marked area in (a) are shown. The Si(1 1 1) planar spacing (3.13 Å) and a planar spacing (2.26 Å) in the gold silicide are seen in (c). This is from a gold silicide island on a bromine-passivated Si(1 1 0) surface. The planar spacing (2.26 Å) is common in gold silicides with a wide range of compositions. See text for details.

of most reported gold silicide structures with a wide range of compositions (Au_2Si to Au_7Si [17] including those mentioned earlier in this paragraph). All of them show the strongest X-ray diffraction peak corresponding to 2.26 Å planar spacing [17]. Neither Au nor Si contain diffraction planes with a planar spacing of 2.26 Å. In the present work, the structures are gold silicides with some composition variation around the Au–Si eutectic composition. The connected bead patterns in Fig. 6 are presumably the result of such a variation in composition as explained earlier.

Scientists working on atomically clean surfaces under ultrahigh vacuum condition may look upon deposition under high vacuum conditions on chemically bromine-passivated substrates as "dirty" systems. However, the fact remains that this "dirty" system has shown results comparable to clean systems [11,12]. After all, in the present case Si supply into the Au layer comes from the purest environment, namely the underlying Si crystal. Additionally, the phenomenon of shape transition, predicted for the clean system [25] has been first observed for this "dirty" system [6]. Now we have shown the growth of many interesting features on bromine-passivated Si(1 1 1) surfaces.

Besides those in Refs. [5–7], there were other cases of interesting growth features on Br–Si(1 1 1) surfaces. Epitaxial Ag layers [26] and nanocrystalline Ge layers [27,28] were also grown on Br–Si(1 1 1) surfaces.

One may wonder, up on annealing, what happens to Br that was initially at the Au/Si interface. This aspect had earlier been studied. Br diffuses out, to some extent behaving like a surfactant in surfactant-mediated growth [22].

For all the interesting results presented here and in our earlier studies of gold silicide growth on Br-passivated Si surfaces, one may wonder if it is necessary to terminate only approximately one-fourth of the Si(1 1 1) dangling bond sites by Br. It should be noted that the saturation of approximately one-fourth of the dangling bonds by Br is obtained *not by choice*. This is what one obtains in the chemical preparation method used. This was analyzed in detail by X-ray standing wave experiments [29–31]. This is apparently due to a steric hindrance arising from the fact that twice the fil-

led-shell radius of Br (r_{Br}) is larger than the distance between two nearest neighbour surface Si atoms (d^{Si}) or between two dangling bonds on an ideal Si(1 1 1) surface. On a Ge(1 1 1) surface the distance between two dangling bonds (d^{Ge}) is larger than twice the filled-shell radius of Br ($2r_{Br} = 3.901$ Å, $d^{Si} = 3.84$ Å, $d^{Ge} = 4.00$ Å), and a larger fraction of dangling bonds have been found to be saturated [32]. On a Si(1 1 1) surface adjacent Br atoms would slightly overlap, thus sterically forbidding termination of more than one-third of the dangling bonds. When Si samples were cleaved in a dilute bromine–methanol solution to obtain Br-passivated Si(1 1 1) surfaces, the maximum termination of the dangling bond sites was 24% [33]. Steric hindrance is also apparently the reason for the inability to obtain Br-passivation of the Si(1 0 0) surface, where there are two dangling bonds per surface Si atom [11,13]. That is why all our growth experiments were performed only on Si(1 1 1) and Si(1 1 0) surfaces. The details of chemical bonding on chemically prepared Br-passivated Si surfaces were studied by X-ray photoelectron spectroscopy and presented in Ref. [13]. We believe all our results would be valid for growth on Br-passivated surfaces where even a larger fraction of dangling bonds would be terminated. Termination of only about one-fourth of the Si(1 1 1) dangling bonds is not a requirement.

4. Conclusions

Thin Au films deposited on Br–Si(1 1 1) substrates and annealed around 363 °C (Au–Si eutectic temperature) with temperature varying between (363 ± 30) °C have produced epitaxial gold silicide islands of various shapes in a self-assembled growth process. It is remarkable that temperature variation over such a small window has produced so rich morphological variations.

Earlier by annealing at the eutectic temperature we obtained equilateral triangular and trapezoidal islands on Si(1 1 1) surfaces. By varying the annealing temperature over a small range around the eutectic temperature, we obtained other shapes of islands expected for growth on a substrate of three-fold symmetry—prominent among them are hexagonal islands, with well defined *facets*. In addition we have observed the growth of ring-like walled hexagonal islands. Observation of chains of connected beads is likely to be due to a phase separation process.

References

[1] Y.M. Mo, B.S. Swartzentruber, R. Kariotis, M.B. Webb, M.G. Lagally, Phys. Rev. Lett. 63 (1989) 2393;
R.J. Hamers, U.K. Kohler, J.E. Demuth, Ultramicroscopy 31 (1989) 10.
[2] M. Bott, T. Michely, G. Comsa, Surf. Sci. 272 (1992) 161.
[3] T. Michely, M. Hohage, M. Bott, G. Comsa, Phys. Rev. Lett. 70 (1993) 3943.
[4] S. Liu, Z. Zhang, G. Comsa, H. Metiu, Phys. Rev. Lett. 71 (1993) 2967.
[5] K. Sekar, G. Kuri, P.V. Satyam, B. Sundaravel, D.P. Mahapatra, B.N. Dev, Surf. Sci. 339 (1995) 96.
[6] K. Sekar, P.V. Satyam, G. Kuri, B. Sundaravel, D.P. Mahapatra, B.N. Dev, Phys. Rev. B 51 (1995) 14330.
[7] B. Rout, B. Sundaravel, A.K. Das, S.K. Ghose, K. Sekar, D.P. Mahapatra, B.N. Dev, J. Vac. Sci. Technol. B 18 (2000) 1847.
[8] K. Sekar, P.V. Satyam, G. Kuri, B. Sundaravel, D.P. Mahapatra, B.N. Dev, Solid State Commun. 96 (1995) 871.
[9] H. Okamoto, T.B. Massalski, Bull. Alloy Phase Diagrams 4 (2) (1983) 190;
W.G. Moffatt, The Handbook of Binary Phase Diagrams, Genium Publishing Corporation, Schenectady, NY, 1986, p. 3/84.
[10] H. Okamoto, D. Chen, T. Tamada, Phys. Rev. Lett. 89 (2002) 256101.
[11] K. Sekar, P.V. Satyam, G. Kuri, D.P. Mahapatra, B.N. Dev, Nucl. Instr. and Meth. B 71 (1992) 308.
[12] K. Sekar, P.V. Satyam, G. Kuri, D.P. Mahapatra, B.N. Dev, Nucl. Instr. and Meth. B 73 (1993) 63.
[13] K. Sekar, G. Kuri, D.P. Mahapatra, B.N. Dev, J.V. Ramana, S. Kumar, V.S. Raju, Surf. Sci. 302 (1994) 25.
[14] J.J. Hoyt, Acta Mater. 47 (1998) 345.
[15] S. Bhattacharyya, T.A. Abinandanan, Bull. Mater. Sci. (India) 26 (2003) 193.
[16] R.C. Krutenat, J.K. Tien, D.E. Ornwalt, Metall. Trans. 2 (1971) 1479.

[17] Joint Committee on Powder Diffraction—International Centre for Diffraction Data (JCPDS—ICDD), 1993.

[18] M. Ellner, Z. Predel, Z. Metallkd. 71 (1980) 364.

[19] G.A. Andersen, J.L. Bestel, A.A. Johnson, B. Post, Mater. Sci. Eng. 7 (1971) 83.

[20] S.S. Lau, B.Y. Tsaur, M. von Allmen, J.W. Mayer, B. Stritzker, C.W. White, B. Appleton, Nucl. Instr. and Meth. 182/183 (1981) 97.

[21] A.K. Green, E. Bauer, J. Appl. Phys. 47 (1976) 1284.

[22] B. Sundaravel, K. Sekar, G. Kuri, P.V. Satyam, B.N. Dev, S. Bera, S.V. Narasimhan, P. Chakraborty, F. Caccavale, Appl. Surf. Sci. 137 (1999) 103.

[23] E. Landree, D. Grozea, C. Collazo-Davila, L.D. Marks, Phys. Rev. B 55 (1997) 7910, and references therein.

[24] B. Sundaravel, K. Sekar, P.V. Satyam, G. Kuri, B. Rout, S.K. Ghose, D.P. Mahapatra, B.N. Dev, Indian J. Phys. A 70 (1996) 687.

[25] J. Tersoff, R.M. Tromp, Phys. Rev. Lett. 70 (1993) 2782.

[26] B. Sundaravel, A.K. Das, S.K. Ghose, K. Sekar, B.N. Dev, Appl. Surf. Sci. 137 (1999) 11.

[27] A.K. Das, S.K. Ghose, B.N. Dev, G. Kuri, T.R. Yang, Appl. Surf. Sci. 165 (2000) 260.

[28] A.K. Das, B.N. Dev, B. Sundaravel, E.Z. Luo, J.B. Xu, I.H. Wilson, Pramana-J. Phys. 59 (2002) 133.

[29] J.A. Golovchenko, J.R. Patel, D.R. Kaplan, P.L. Cowan, M.J. Bedzyk, Phys. Rev. Lett. 49 (1982) 560.

[30] P.L. Cowan, J.A. Golovchenko, M.F. Robbins, Phys. Rev. Lett. 44 (1980) 1680.

[31] M.J. Bedzyk, W.M. Gibson, J. Vac. Sci. Technol. 20 (1982) 632.

[32] M.J. Bedzyk, G. Materlik, Phys. Rev. B 31 (1985) 4110.

[33] B.N. Dev, V. Aristov, N. Hertel, T. Thundat, W.M. Gibson, Surf. Sci. 163 (1985) 457.